Statistical inference of the ice velocity response to meltwater runoff, terminus position, and bed topography at Helheim Glacier, Greenland

Lizz Ultee[1], Denis Felikson[2], Brent Minchew[1], Leigh A Stearns[3], and Bryan Riel[1]

[1]Massachusetts Institute of Technology
[2]NASA Goddard Space Flight Center
[3]University of Kansas

November 24, 2022

Abstract

The Greenland Ice Sheet discharges ice to the ocean through hundreds of outlet glaciers.
Recent acceleration of Greenland outlet glaciers has been linked to both oceanic and atmospheric drivers.
Here, we leverage temporally dense observations, regional climate model output, and newly developed time series analysis tools to assess the most important forcings causing ice flow variability at one of the largest Greenland outlet glaciers, Helheim Glacier, from 2009 to 2017. We find that ice speed correlates most strongly with catchment-integrated runoff at seasonal to interannual scales, while multi-annual flow variability correlates most strongly with multi-annual terminus variability. The multiple relevant time scales and the influence of subglacial topography on Helheim Glacier's dynamics highlight different regimes that can inform modeling and forecasting of its future. Notably, our results suggest that the recent terminus history observed at Helheim is a response to, rather than the cause of, upstream changes.

Posted on 24 Nov 2022 — CC-BY-NC 4 — https://doi.org/10.1002/essoar.10506878.1 — This a preprint and has not been peer reviewed. Data may be preliminary.

Statistical inference of the ice velocity response to meltwater runoff, terminus position, and bed topography at Helheim Glacier, Greenland

Lizz Ultee[1,2], Denis Felikson[3], Brent Minchew[1], Leigh A. Stearns[4], Bryan Riel[1]

[1]Dept. of Earth, Atmospheric, and Planetary Sciences, Massachusetts Institute of Technology, Cambridge, MA, USA
[2]School of Earth & Atmospheric Sciences, Georgia Institute of Technology, Atlanta, GA, USA
[3]NASA Goddard Space Flight Center, Greenbelt, MD, USA
[4]Department of Geology, University of Kansas, Lawrence, KS, USA

Key Points:

- Multiple variables control the ice velocity of Helheim Glacier, Greenland.
- At seasonal timescales, ice velocity responds most strongly to catchment-integrated meltwater runoff.
- Glacier terminus position is an important control on velocity only at multi-annual timescales.

Corresponding author: Lizz Ultee, `ehultee@umich.edu`

Abstract

The Greenland Ice Sheet discharges ice to the ocean through hundreds of outlet glaciers. Recent acceleration of Greenland outlet glaciers has been linked to both oceanic and atmospheric drivers. Here, we leverage temporally dense observations, regional climate model output, and newly developed time series analysis tools to assess the most important forcings causing ice flow variability at one of the largest Greenland outlet glaciers, Helheim Glacier, from 2009 to 2017. We find that ice speed correlates most strongly with catchment-integrated runoff at seasonal to interannual scales, while multi-annual flow variability correlates most strongly with multi-annual terminus variability. The multiple relevant time scales and the influence of subglacial topography on Helheim Glacier's dynamics highlight different regimes that can inform modeling and forecasting of its future. Notably, our results suggest that the recent terminus history observed at Helheim is a response to, rather than the cause of, upstream changes.

Plain Language Summary

Hundreds of "outlet glaciers" transport ice from the Greenland Ice Sheet to the ocean. The flow of those outlet glaciers has sped up in recent decades, increasing the contribution of Greenland ice to global mean sea-level rise. Previous studies suggest that changes in both the ocean and the atmosphere could cause the observed speedup. In this study, we bring together satellite observations and information from a regional climate model with new software tools to determine which factors in an outlet glacier system are the most likely causes of velocity variation. Based on previous studies, we might expect ocean-driven changes to be the dominant cause of velocity variation for Helheim Glacier. Instead, we find that the most important factors differ at different time scales. Velocity changes over the course of a few months to a year respond to variations in the amount of meltwater in the glacier system, which depends on atmospheric conditions. Over longer time scales, velocity changes respond more strongly to the position of the glacier front, where it meets the ocean. The interaction of multiple factors across time scales highlights the importance of continued efforts to simulate future changes of large Greenland outlet glaciers in detail.

1 Introduction

In recent decades, several glaciers draining the Greenland Ice Sheet have accelerated, increasing their contribution to global mean sea-level rise (Rignot & Kanagaratnam, 2006; Rignot et al., 2011; Bevan et al., 2012). The observed acceleration of outlet glaciers and the ice sheet interior has been attributed to warmer ocean waters melting glacier fronts (Murray et al., 2010; Rignot et al., 2012) as well as increased surface melt (Joughin et al., 2008; Doyle et al., 2014). Numerical models and indirect observations indicate that increasing runoff could enhance solid ice loss by lubricating the glacier bed and warming the ice such that it deforms more readily (Reeh & Olesen, 1986; Krabill et al., 1999; Parizek & Alley, 2004; Phillips et al., 2010; Poinar et al., 2017). However, in situ observations of the Greenland Ice Sheet margin have found limited evidence for annual-scale acceleration of ice flow driven by increasing runoff (Stevens et al., 2016; Nienow et al., 2017). At marine outlets including Helheim Glacier, observations show that ice flow speed (and therefore mass discharge) correlates most strongly with iceberg calving activity rather than runoff (Howat et al., 2005; Joughin et al., 2008; Nettles et al., 2008; Kehrl et al., 2017; Vijay et al., 2019).

Helheim Glacier is currently the highest-flux outlet of the Greenland Ice Sheet (Mankoff et al., 2019). Its dynamics through the early 21st century showed pronounced variability, including episodes of multi-annual retreat and readvance (Howat et al., 2005, 2007; Bevan et al., 2012) and net mass gain while most Greenland outlet glaciers were losing mass (Howat et al., 2011). Sediment records from the past century suggest that Helheim responds to atmospheric and oceanic variability on time scales of a few years (Andresen et al., 2012), highlighting the importance of understanding its dynamics on sub-annual to multi-annual time scales. The high ice flux through Helheim Glacier (Rignot et al., 2004; Mankoff et al., 2019), its recent variability (Stearns & Hamilton, 2007; Howat et al., 2005, 2007), and its sensitivity to short-term variation in climate forcings (Nick et al., 2009; Andresen et al., 2012) motivate a quantitative comparison of hypothesized controls on velocity variability.

Processes contributing to velocity variability operate at different time scales. For example, fracture-driven changes in stress balance can be nearly instantaneous and propagate rapidly, shaping velocity on the order of hours to days (Das et al., 2008; Nettles et al., 2008; Cassotto et al., 2019), while changes in the subglacial drainage system may take days to months (Meier et al., 1994; Kamb et al., 1994; Shepherd et al., 2009; Bartholomew et al., 2010; Pimentel & Flowers, 2011) and response to changing upstream snow accumulation can take many years (Weertman, 1958; Nye, 1960; van der Veen, 2001). Observations that permit a detailed understanding of one process – such as intensive field study of a calving front – may not be sufficient to contextualize influences from processes operating at other scales. Accounting for the relative influence of each process, for example to develop accurate predictive models, requires synthesising observations and inference across scales. Here, we apply the flexible time series analysis tools developed by Riel et al. (2021) to publicly available velocity fields (Joughin et al., 2020) and correlate the results with temporally dense climate model output (Van Meijgaard et al., 2008; Noël et al., 2018) and terminus observations (Supplementary Material) to study the forcings of and responses to velocity variability at Helheim over multiple temporal scales.

2 Methods

2.1 Inference framework

We investigate correlations between surface velocity and several factors hypothesized to drive its variability at seasonal to multi-annual scales. Figure 1 shows the system of causal connections we investigate here. Limited time-dependent data precludes us from studying the effect of ice mélange, ocean temperature, and surface damage directly. Here, we assume that the primary effect of those three variables is on the rate of calving, and we restrict the present study to the relationship between glacier terminus position and surface ice velocity. We focus our analysis on time scales of months to years. As such, we do not consider the flow response to individual calving events (Murray et al., 2015) or tidal variation (de Juan et al., 2010; Voytenko et al., 2015), which have been described elsewhere.

We investigate three factors varying in time (surface mass balance, runoff, and width-averaged terminus position) and one varying in space (subglacial topography). To quantify the strength of the temporal variables' relationship with velocity, we compute their cross-correlation as described below. We interpret the qualitative effect of local topography on velocity variation by analysing spatial patterns in the cross-correlations computed for the temporal variables.

2.2 Catchment data

We produce a one-dimensional time series for each catchment variable. We integrate monthly surface mass balance and runoff derived from Noël et al. (2018) over the Helheim Glacier catchment defined by Mankoff et al. (2020). The time series of calving front position is a width-averaged distance from an upstream flux gate, identified from satellite imagery (Supplementary Dataset S1) with variable temporal resolution. For the present study of seasonal to multi-annual time scales, we apply a 10-day smoothing window to the terminus record. We trim all time series to the period for which data is avail-

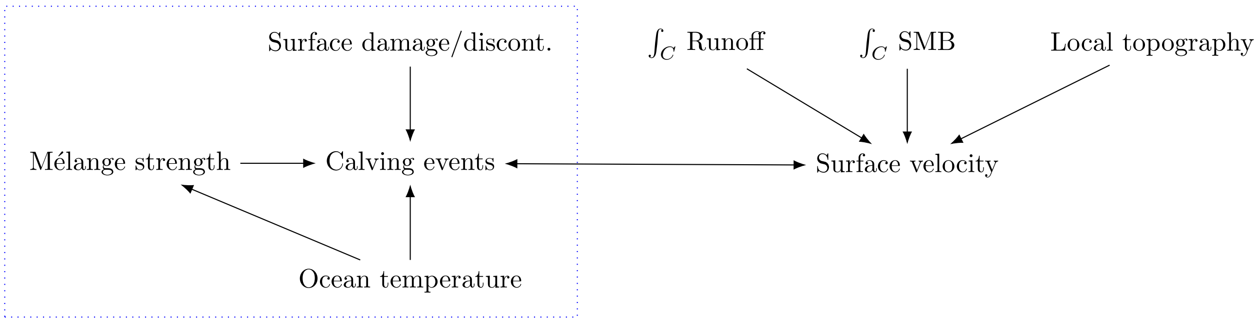

Figure 1. Causal relationships tested in this work. Surface mass balance (SMB) and runoff are catchment-integrated quantities ($\int_C$), both from (Noël et al., 2018). Surface velocity from (Joughin et al., 2020) is evaluated at each point. We use terminus position from satellite imagery (Section 2.2) as a proxy for all ocean-driven processes (blue dotted box)

able for all variables: 2009-2017. We interpolate a piecewise linear time-continuous function for each time series using the Interp1d class of SciPy v1.4.1 (Virtanen et al., 2020).

2.3 Producing temporally continuous velocity functions

We use frequent observations and spline interpolation to produce time-continuous estimates of ice surface velocity. We stack all available InSAR-derived glacier site velocity observations from Joughin et al. (2020) and extract 1-dimensional time series of velocity at points spaced at 1 km intervals along a central flowline (as defined in Felikson et al., 2021). We define an upstream limit to our analysis by the area for which there are sufficient velocity observations to constrain a time-continuous fit. The selected points are shown in Figure 2A-B.

We then construct a continuous function that best fits the observed values at each point. Following Riel et al. (2021), we perform a regularized least squares regression that estimates the optimal linear combination of representative time functions (linear polynomials, B-splines, and integrated B-splines of pre-defined center times and scales) to fit the data at each point. The resulting function is an optimized superposition of linear trend, seasonal variability, and secular change, which facilitates later decomposition into components of interest. Example observations and constructed continuous functions are shown in Figure 2C.

2.4 Normalized cross-correlation

Finally, we find and compare the cross-correlations describing ice speed response to each variable at each point. We sample each time-continuous function at regular intervals. Dickey-Fuller and KPSS tests applied using the Python package statsmodels v0.12.2 (Seabold & Perktold, 2010) indicate that the raw time series are non-stationary — that is, their means and/or variances change over time, which can produce spurious results in cross-correlation analysis (Shumway & Stoffer, 2017). In sections 3.1-3.2, we enforce stationarity by differencing:

$$f_i = \hat{f}_i - \hat{f}_{i-1}, \qquad (1)$$

where $\hat{f}_i$ is the i^{th} point in the raw time series and f is the differenced time series. We elect not to difference the long-term-varying series tested in section 3.3, as doing so would remove the signal of interest.

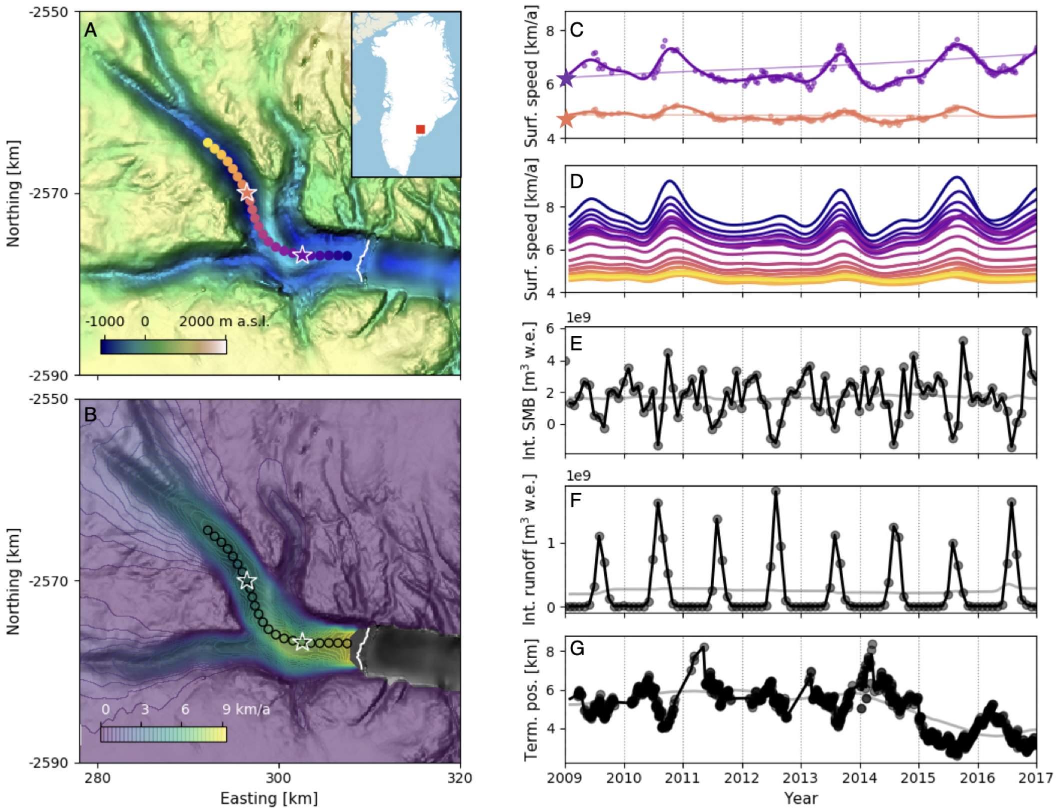

Figure 2. The physical setting of Helheim Glacier studied here. (A) Hillshade map of Helheim Glacier subglacial topography from Morlighem et al. (2017) with 2009 terminal edge from Joughin et al. (2020) in white, points along central flowline in bright colors, and inset map of Helheim Glacier location within Greenland; (B) Mean ice surface speed as of 2016 (ENVEO, 2017), with flowline points outlined; (C) Ice surface speed at two locations from Joughin et al. (2020) (points) and B-spline smooth approximation to each time series (curves); (D) B-spline continuous velocity functions for each point along the flowline in panel A, with curve color indicating which point is represented; (E) Catchment-integrated surface mass balance from RACMO; (F) Catchment-integrated runoff from RACMO (Noël et al., 2018); and (G) Width-averaged terminus position, relative to a fixed gate on the glacier (larger numbers indicate advance). In panels E-G, data from the original source is plotted as points, and dark lines show the values of 1d-interpolated functions used to determine signal cross-correlation. In panels C and E-G, light curves show the long-term-varying component of each signal.

We compute the normalized cross-correlation at lag k,

$$XCorr(f, v)_k = \frac{1}{N}\sum_{i=1}^{N} \frac{f_{i+k} - \bar{f}}{\sigma(f)} \frac{v_i - \bar{v}}{\sigma(v)}, \quad (2)$$

for $k \in [-N, N]$, where ice speed v and variable f are each time series of length N, differenced as in Eqn. 1, with means $(\bar{v}, \bar{f})$ and standard deviations $(\sigma(v), \sigma(f))$. With this convention, a lag $k < 0$ refers to a cross-correlation with the velocity series offset backward in time; that is, strong cross-correlations at negative lag indicate that a change is observed first in the velocity signal and a similar change is observed later in the variable f signal. The normalized cross-correlation may take values between ± 1, and a cross-correlation at lag k is statistically significant at the 95% confidence level if it exceeds $1.96/\sqrt{N-k}$.

Because we anticipate multiple influences on observed surface velocity (Figure 1), we do not expect the magnitude of correlations to be close to 1. Rather, we identify the largest-magnitude statistically significant correlations for each variable at each point, and we compare their relative strength. From the full time series (Section 3.1) and then from annual subsets (Section 3.2) and from series filtered to show only multi-annual variability (Section 3.3), we identify the largest magnitude of cross-correlation between the series and the lag in days at which that extreme value occurs. We analyse both positive and negative lag times for terminus position, given the bidirectional causal relationship we expect for that variable (Figure 1). We restrict our analysis to positive lag values for surface mass balance and runoff. The quasi-periodic nature of those signals is likely to produce significant cross-correlations at negative lags, but there is no physical reason to expect feedbacks from velocity to mass balance or runoff at seasonal to multi-annual time scales.

3 Results

3.1 Seasonal to interannual velocity variability responds most strongly to runoff

The normalized, single-differenced cross-correlations with ice surface speed are distinct for each variable. The weakest cross-correlations along the flowline, on average, are with catchment-integrated surface mass balance (Fig. 3, left column). For that variable, the strongest negative correlation is -0.17, found at the farthest downstream point. The strongest positive correlation is 0.13, found 14 km upstream. Cross-correlation of ice surface speed with catchment-integrated runoff (Fig. 3, center column) is stronger. Its peak positive value is 0.25, found near the terminus, and its strongest negative value is -0.20, found 19 km upstream. Terminus position (Fig. 3, right column) also shows comparatively strong cross-correlations with velocity. The strongest correlation is -0.22, found near the terminus, and the strongest positive correlation is 0.19, found 14 km upstream from the terminus. However, the strongest cross-correlations are found at negative lags, suggesting that terminus position is responding to upstream velocity variation rather than vice versa.

At every point, the magnitude of strongest cross-correlation with velocity is larger for runoff than for surface mass balance, on average 1.2 times larger over the flowline. The cross-correlation between terminus position and velocity is similar in magnitude to that of runoff, but the former appears to be a response to velocity changes while the latter leads velocity changes. We infer that runoff exerts the strongest control on seasonal to interannual ice surface velocity variability along the main trunk of Helheim Glacier.

3.2 No year in which terminus position is more important than runoff

Because Helheim Glacier is a complex system that changes over time, the multi-year bulk analysis of section 3.1 may not capture important interannual changes in the

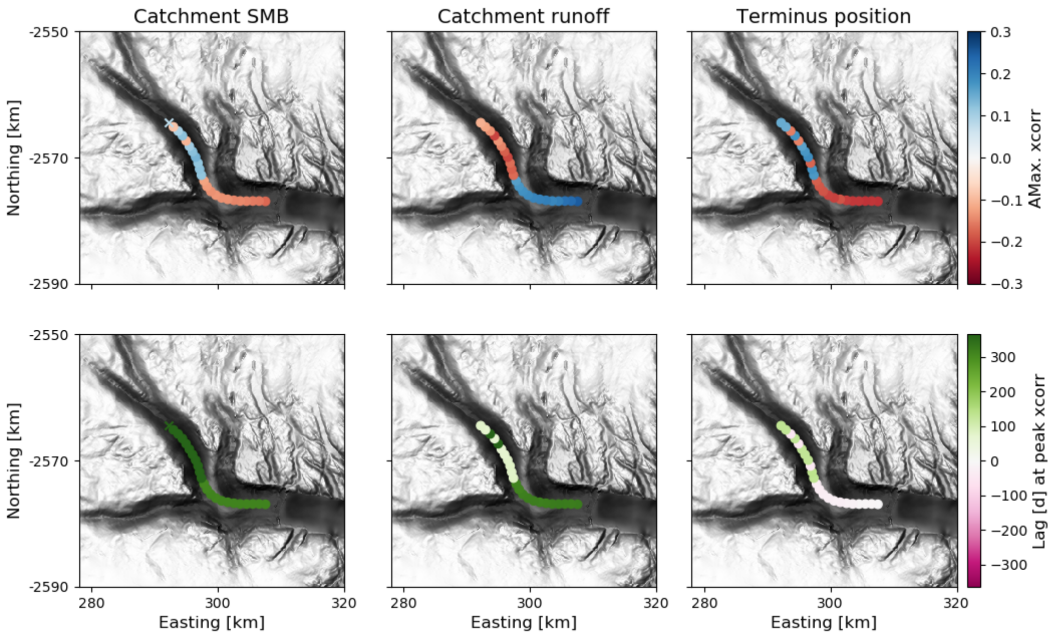

Figure 3. The cross-correlation of largest absolute value ("AMax. xcorr") (top row) between ice surface speed and each variable (columns), and the lag in days (bottom row) at which that cross-correlation is found. Circles and crosses indicate values that are and are not significant at the 95% confidence level, respectively.

dominant sources of its velocity variability. To study year-to-year changes in more detail, we computed the cross-correlation between single-year subsets of the variables we studied in section 3.1. Cross-correlations of these single-year subsets are generally stronger than those found over the full time period. We present both positive and negative lags for all variables, as the signals are quasi-periodic.

The patterns of cross-correlation between single-year sections of the signals vary from year to year, as shown in Figure 4. For example, in 2009 the cross-correlation between runoff and surface speed at a downstream point is strongest at a lag of around 90 days, with a statistically significant minimum following at longer lag times. In 2010, 2012, and 2013, the strongest correlation between runoff and surface speed is in negative lag space, which we interpret as a response to past years' runoff peaks. There are statistically significant correlations between runoff and surface speed every year.

We find that the normalized cross-correlation of terminus position and ice surface speed is generally low. That correlation is statistically significant in only four of the eight years we analyse. The strongest of those correlations are in 2010 and 2013, where there is a significant correlation for small negative lags, indicating that terminus position changed in response to a velocity change. For every year we study, ice surface speed correlates much more strongly with catchment-integrated runoff than with terminus position.

3.3 Multi-annual velocity variability correlates with terminus position

We apply a boxcar filter with window of 2 years to the surface mass balance, runoff, and terminus position data to isolate long-term (multi-annual) from shorter-term variability. We then extract the long-term-varying signal from the ice speed timeseries as discussed in Section 2.3. The isolated long-term components are shown as light curves in Figure 2. Finally, we recompute the cross-correlation for the filtered time series.

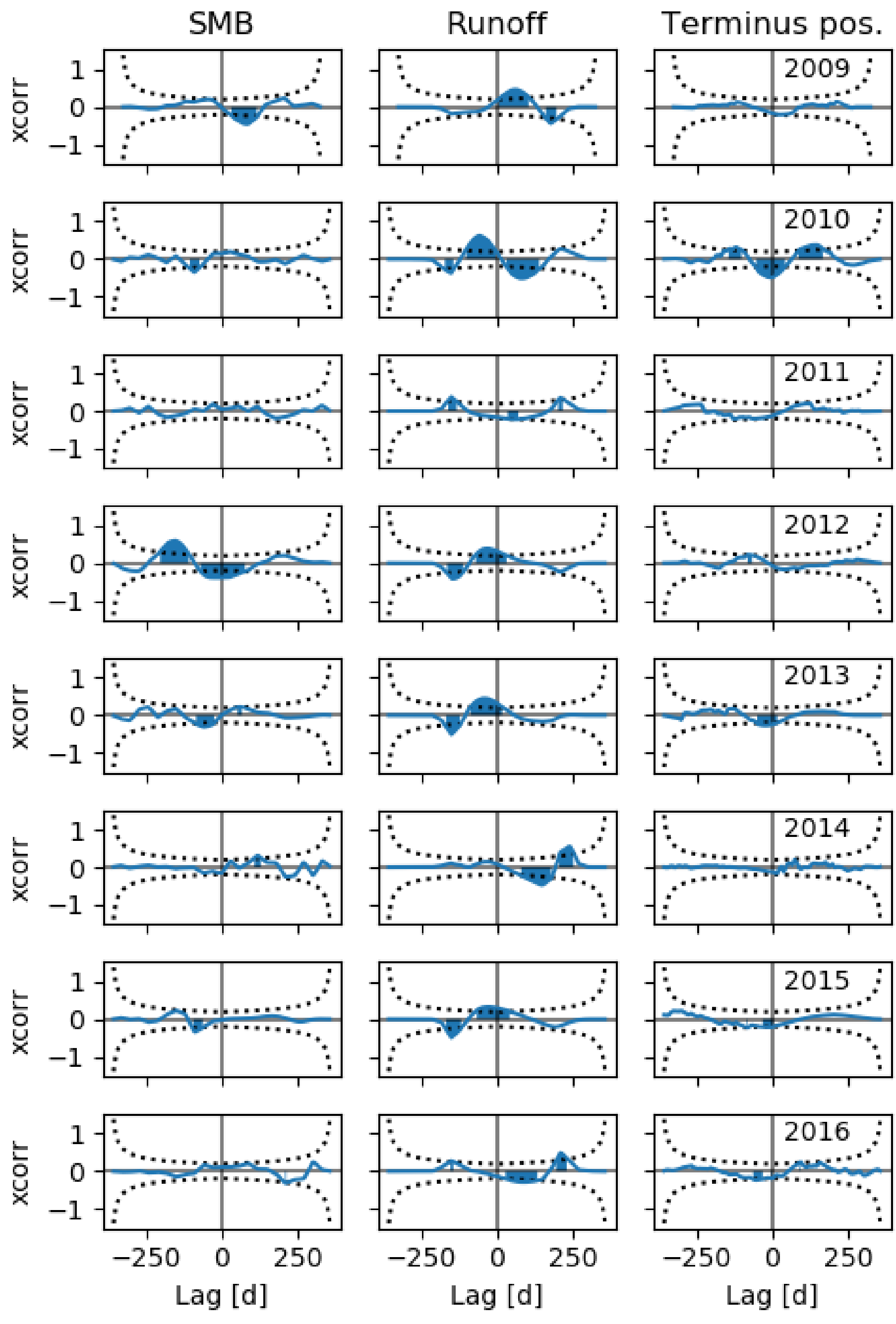

Figure 4. Annual patterns of cross-correlation between surface speed and system variables for (left) surface mass balance, (center) runoff, and (right) terminus position, sampled at a point 5 km upstream from the 2009 terminus. Dotted curves indicate 95% confidence intervals around $XCorr(f, v) = 0$; shading indicates statistically significant difference from zero.

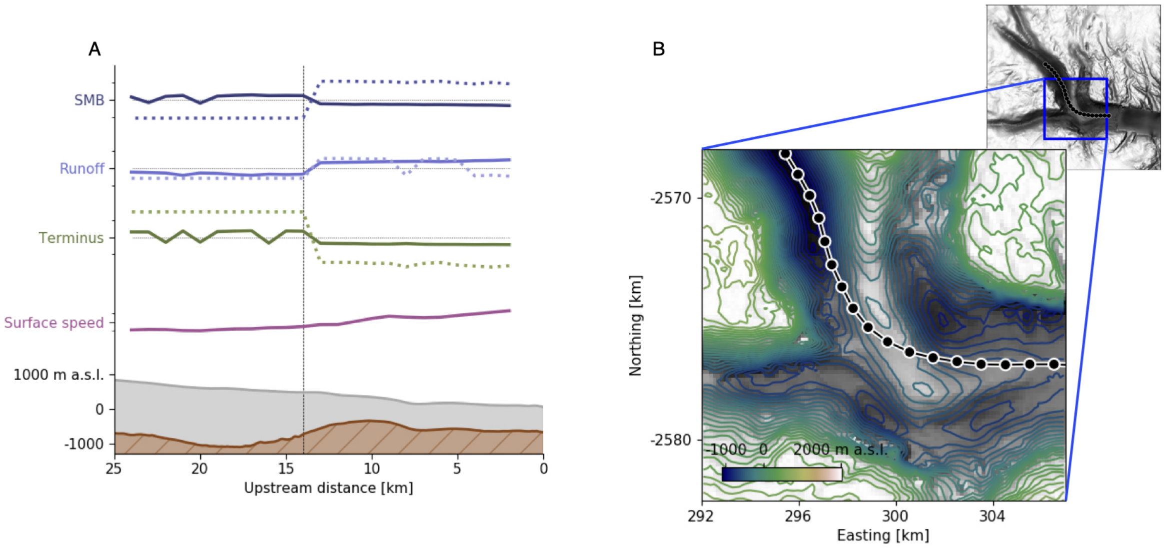

Figure 5. Influence of a subglacial ridge on Helheim Glacier dynamics. A) Ice speed cross-correlation with each variable tested, for each point along the flowline, vertically offset for legibility. Variable labels coincide with zero cross-correlation and minor ticks indicate $XCorr(f, v) = \pm 0.5$. Solid lines are cross-correlations of the full signals (as reported in Figure 3 and Section 3.1). Dashed lines show results filtered to isolate long-term variability (as in Section 3.3 and Figure S1). Lower portion shows bed topography (brown), ice surface (grey), and mean surface speed (purple) along the flowline. Velocity ticks correspond to 4.5, 6.0, and 7.5 km a^{-1}. Vertical marker indicates position of sign changes in cross-correlation for multiple variables. B) Enlarged contour map of the Helheim Glacier trough around the bedrock bump. Background image is a black and white hillshade of the topography as in Figure 3; contours show intervals of approximately 60 meters elevation. Contour colormap and flowline points (black) are consistent with Figure 2A.

We see a strong correlation between the long-term-varying components of ice speed and terminus position. The correlation between these two component signals is much stronger than between the corresponding full signals (Figures 5 and S1), with values along the lower trunk averaging -0.8, all for non-negative lags. A cross-correlation stronger than that for the full signals is also seen for long-term-varying surface mass balance, ranging from -0.54 to 0.54. The correlation between long-term-varying components of ice speed and runoff is comparable to that between the full signals, ranging from -0.29 to 0.29. We infer that terminus position variability is most important for Helheim Glacier's dynamics at multi-annual time scales.

3.4 Subglacial topography modulates velocity response to each variable

The flowline we examine flows through a trough with a pronounced ridge in its subglacial topography. The ridge creates a steep along-flow thickness gradient as well as a lateral constriction (Figure 5). For all three variables, the flowline separates into two segments with opposite sign of maximum cross-correlation. We find changes in sign of absolute maximum cross-correlation with velocity at 14 km upstream from the terminus—coincident with the upstream edge of the subglacial ridge (Figures 3, 5, and S1). We also find step changes in the lag at which the strongest cross-correlation occurs aligned with the ridge. The spatial pattern of cross-correlation is similar for both seasonal and multi-annual signals (Sections 3.1-3.3). These patterns suggest that the dynamics of the upstream and downstream segments of the flowline are fundamentally different from one another. We interpret that the bedrock ridge is an obstacle to the propagation of traveling waves (Nye, 1960; Fowler, 1982; Weertman & Birchfield, 1983)—whether the waves carry velocity variability, seasonal runoff input, or stress adjustment to terminus change or surface mass balance.

4 Discussion

Our analysis illustrates that Helheim Glacier is a dynamic system with more than one important control on its velocity. We find that seasonal-scale variations in ice surface speed correlate more strongly with catchment-integrated runoff than with terminus position, for the full period 2009-2017 (Figure 3) and for every year in it (Figure 4). At the multi-annual scale we find stronger correlation with terminus position than with runoff (Figure 5), consistent with the findings of Vijay et al. (2019), and in agreement with earlier work relating ice velocity to ice thickness and glacier terminus position on Alaskan tidewater glaciers (Meier & Post, 1987; O'Neel et al., 2005). Our results support previous findings that increasing meltwater supply can enhance seasonal speedups in ice flow, but does not contribute to multi-annual acceleration (summarized in Nienow et al., 2017). Our analysis also supports the assessment by Enderlin et al. (2018) that hypothesised distinct variables driving different timescales of velocity variability at Columbia Glacier, Alaska.

The correlation of runoff with seasonal-scale velocity variation described in Section 3.1 is consistent with observations of land-terminating margins of the Greenland Ice Sheet (Joughin et al., 2008) and some marine outlets on Greenland's west coast (Sole et al., 2011; Moon et al., 2015), as well as inference of surface-melt-induced acceleration (Andersen et al., 2011) and dynamic thinning (Bevan et al., 2015) at Helheim. Although our conclusions differ from Moon et al. (2014) and Vijay et al. (2019), who infer that terminus changes are the strongest control on Helheim's velocity, the observations presented in those studies are consistent with our interpretation that seasonal variations in ice surface speed are more strongly correlated with runoff than with terminus position change. In agreement with Kehrl et al. (2017), we find that 2010 and 2013 are the years for which ice surface speed at Helheim is most correlated with terminus position (Fig. 4). However, our quantitative analysis shows that, in all years, Helheim's speed is more correlated with runoff than terminus position.

The relative importance of each driver at Helheim Glacier likely does not translate to other outlets or other time periods. For example, our findings at Helheim contrast those of King et al. (2020), who found that regionally aggregated trends in Greenland Ice Sheet discharge correlated most strongly to glacier front position. Ice velocity at Helheim may be unusually sensitive to catchment-integrated runoff because of the presence of a large firn aquifer that allows hydrofracturing of deep crevasses and enhances deformational ice motion (Poinar et al., 2017; Miller et al., 2020). The lower trunk of the glacier was also near flotation during the time period we study here (Kehrl et al., 2017), which could render it especially sensitive to both changing basal water pressure (runoff) and calving activity (Andersen et al., 2010; Cassotto et al., 2019). Finally, the spatial pattern of our results highlights the role of unique subglacial topography in shaping the dynamic response to forcing (Enderlin et al., 2013; Khan et al., 2014; Felikson et al., 2017; Catania et al., 2018; Enderlin et al., 2018; Felikson et al., 2021). Although our results may be unique to Helheim during the 2009-2017 period, our methods can be applied to investigate any glacier with a sufficient observational record.

One explanation for the weak correlation between ice surface speed and terminus position throughout our study period is that the sensitivity of surface speed to terminus position is itself determined by the terminus position (Cassotto et al., 2019), and that the terminus did not reach a hypothetical critical position during the time we observed. From 2009-2014, the observed terminus positions oscillated around a steady mean position at approximately 6 km forward of our reference position; a period of multi-annual retreat beginning in late 2014 reflects a multi-annual acceleration on the lower glacier trunk beginning around the same time (Figure 2D and G). If the terminus had reached a critical position that increased the sensitivity of surface speed to terminus change, we would expect to see change in the correlation between those variables as terminus position changed over time. Instead we find that the annual cross-correlation between surface speed and terminus position is no stronger in 2015 and 2016 than in previous years (Figure 4).

A second explanation for the weak correlation between ice surface speed and terminus position is that iceberg calving is episodic and discontinuous. Field observations of Helheim Glacier at finer temporal scales than we study here have found that calving activity was an important control on velocity at the timescale of minutes to hours (Nettles et al., 2008; de Juan et al., 2010), and that runoff during the melt season contributes to daily velocity increases (Andersen et al., 2010, 2011). Thus, even with our temporally dense records—average 3 days between measurements—we may more realistically expect to see responses to runoff than to iceberg calving. Further, we analyse a width-averaged terminus position, which will not capture differing dynamic responses to iceberg calving at different points along the face. Extending our methodology to analyse the fine spatial and temporal scales captured in field observations could provide a fuller picture of the forcings driving velocity variability (building on Podrasky et al., 2012, for example).

In this work, we have assumed that terminus position evolves independently from catchment-integrated runoff (Figure 1). This choice ignores the established connection between calving rate and subglacial discharge at the terminus (Bartholomaus et al., 2013; Cook et al., 2014; Slater et al., 2015; Fried et al., 2018; van Dongen et al., 2020). Modelling efforts suggest that the calving response to subglacial discharge depends on the subglacial hydrologic system near the terminus, in particular whether melt is localized to channels (Slater et al., 2015; Todd et al., 2018; van Dongen et al., 2020). Subglacial discharge also affects calving through its influence on the vertical pattern of submarine melt (Motyka et al., 2003; Jenkins, 2011; O'Leary & Christoffersen, 2013; Luckman et al., 2015; Slater et al., 2015; Ma & Bassis, 2019). Recent observations have found no evidence for a melt-induced enhancement of calving at Helheim Glacier, perhaps because of its broad and deep terminus (Everett et al., 2021). However, we anticipate that accounting for a connection between runoff and calving activity would further strengthen the apparent role of runoff in setting Helheim Glacier surface velocity. As new observations of the near-terminus environment become available, future work may apply multivariate statistical methods to assess this prediction quantitatively.

Our results show that numerical ice flow modeling experiments will require multiple forcing mechanisms to capture the dynamics of Helheim Glacier. Several state-of-the-art studies, including the standard experiments performed by several numerical models as part of the the Ice Sheet Modeling Intercomparison for the Coupled Model Intercomparison Project Phase 6 ('ISMIP6", Nowicki et al., 2020), have used projections of outlet glacier terminus positions to force Greenland Ice Sheet mass change simulations (Choi et al., 2017; Morlighem et al., 2019). Our results show that this approach is a good strategy for projections of multi-annual changes of glaciers like Helheim. However, if future ice sheet modeling efforts seek to reproduce seasonal velocity changes, runoff forcing must be included. The continued development of subglacial hydrology models (Pimentel & Flowers, 2011; Werder et al., 2013) and efforts to couple them with ice dynamics models (Aschwanden et al., 2016; Brinkerhoff et al., 2021) are therefore vital to refining our understanding of the future evolution of the Greenland Ice Sheet.

5 Conclusions

We have computed normalized cross-correlations between three catchment variables (surface mass balance, runoff, and terminus positions) and ice surface velocity of Helheim Glacier, revealing the dominant controls on velocity variability at multiple time scales. We find that velocity responds most strongly to catchment-integrated runoff at seasonal scale. At multi-annual scale, velocity variability shows stronger correlation with terminus position change. We find distinct patterns in correlation along upstream and downstream portions of the glacier trunk, separated by a subglacial ridge. The time scale separation of major sources of variability, and the role of underlying topography, are important considerations in designing numerical ice flow simulators to project the future evolution of large outlet glaciers.

Acknowledgments
LU designed the study, with input from DF and BM. DF gathered model data and contributed literature review. LS contributed a dense record of satellite-derived terminus positions. BR developed software used to construct time-continuous velocity functions. LU performed quantitative analysis and produced manuscript figures. LU and DF drafted the manuscript, and all authors contributed to editing and approving its final form.

Work toward this manuscript was supported by the National Aeronautics and Space Administration grant NNX16AJ90G and Heising Simons Foundation grant 2017-316.

All code used in this analysis is available via GitHub and archived on Zenodo. Construction of the time-continuous velocity functions: `https://doi.org/10.5281/zenodo.4474829`. Along-flowline data extraction and cross-correlation: `https://doi.org/10.5281/zenodo.4707999`. Data pre-processing and visualization: `https://doi.org/10.5281/zenodo.4707997`. Terminus position data is available as a supplement to this manuscript and [will be deposited] in the Dryad data repository.

The authors thank Brice P. Y. Noël for providing RACMO surface mass balance data and discussing its processing. LU thanks Jeremy Bassis for long-ago chats about inference on weighted directed graphs, which percolated into Figure 1.

References

Andersen, M. L., Larsen, T. B., Nettles, M., Elosegui, P., van As, D., Hamilton, G. S., … Dahl-Jensen, D. (2010). Spatial and temporal melt variability at Helheim Glacier, East Greenland, and its effect on ice dynamics. *Journal of Geophysical Research: Earth Surface*, *115*(F4). doi: 10.1029/2010JF001760

Andersen, M. L., Nettles, M., Elosegui, P., Larsen, T. B., Hamilton, G. S., & Stearns, L. A. (2011). Quantitative estimates of velocity sensitivity to surface melt variations at a large Greenland outlet glacier. *Journal of Glaciology*, *57*(204), 609-620. doi: 10.3189/002214311797409785

Andresen, C. S., Straneo, F., Ribergaard, M. H., Bjørk, A. A., Andersen, T. J., Kuijpers, A., … Ahlstrøm, A. P. (2012). Rapid response of Helheim Glacier in Greenland to climate variability over the past century. *Nature Geoscience*, *5*(1), 37–41. doi: 10.1038/ngeo1349

Aschwanden, A., Fahnestock, M. A., & Truffer, M. (2016). Complex Greenland outlet glacier flow captured. *Nature Communications*, *7*, 10524 EP. doi: 10.1038/ncomms10524

Bartholomaus, T. C., Larsen, C. F., & ONeel, S. (2013). Does calving matter? Evidence for significant submarine melt. *Earth and Planetary Science Letters*, *380*, 21–30. doi: 10.1016/j.epsl.2013.08.014

Bartholomew, I., Nienow, P., Mair, D., Hubbard, A., King, M. A., & Sole, A. (2010). Seasonal evolution of subglacial drainage and acceleration in a Greenland

outlet glacier. *Nature Geoscience*, *3*(6), 408–411. doi: 10.1038/ngeo863
Bevan, S. L., Luckman, A., Khan, S. A., & Murray, T. (2015). Seasonal dynamic thinning at Helheim Glacier. *Earth and Planetary Science Letters*, *415*, 47–53. doi: 10.1016/j.epsl.2015.01.031
Bevan, S. L., Luckman, A. J., & Murray, T. (2012). Glacier dynamics over the last quarter of a century at Helheim, Kangerdlugssuaq and 14 other major Greenland outlet glaciers. *The Cryosphere*, *6*(5), 923–937. doi: 10.5194/tc-6-923-2012
Brinkerhoff, D., Aschwanden, A., & Fahnestock, M. (2021). Constraining subglacial processes from surface velocity observations using surrogate-based Bayesian inference. *Journal of Glaciology*, 1-19. doi: 10.1017/jog.2020.112
Cassotto, R., Fahnestock, M., Amundson, J. M., Truffer, M., Boettcher, M. S., De La Peña, S., & Howat, I. (2019). Non-linear glacier response to calving events, Jakobshavn Isbræ, Greenland. *Journal of Glaciology*, *65*(249), 39-54. doi: 10.1017/jog.2018.90
Catania, G. A., Stearns, L. A., Sutherland, D. A., Fried, M. J., Bartholomaus, T. C., Morlighem, M., … Nash, J. (2018). Geometric controls on tidewater glacier retreat in central western Greenland. *Journal of Geophysical Research: Earth Surface*, *123*(8), 2024-2038. doi: 10.1029/2017JF004499
Choi, Y., Morlighem, M., Rignot, E., Mouginot, J., & Wood, M. (2017). Modeling the response of Nioghalvfjerdsfjorden and Zachariae Isstrøm glaciers, Greenland, to ocean forcing over the next century. *Geophysical Research Letters*, *44*(21), 11,071–11,079. doi: 10.1002/2017GL075174
Cook, S., Rutt, I. C., Murray, T., Luckman, A., Zwinger, T., Selmes, N., … James, T. D. (2014). Modelling environmental influences on calving at Helheim Glacier in eastern Greenland. *The Cryosphere*, *8*(3), 827–841. doi: 10.5194/tc-8-827-2014
Das, S. B., Joughin, I., Behn, M. D., Howat, I. M., King, M. A., Lizarralde, D., & Bhatia, M. P. (2008). Fracture propagation to the base of the Greenland Ice Sheet during supraglacial lake drainage. *Science*, *320*(5877), 778–781. doi: 10.1126/science.1153360
de Juan, J., Elósegui, P., Nettles, M., Larsen, T. B., Davis, J. L., Hamilton, G. S., … Forsberg, R. (2010). Sudden increase in tidal response linked to calving and acceleration at a large Greenland outlet glacier. *Geophysical Research Letters*, *37*(12). doi: 10.1029/2010GL043289
Doyle, S. H., Hubbard, A., Fitzpatrick, A. A. W., van As, D., Mikkelsen, A. B., Pettersson, R., & Hubbard, B. (2014, 2021/02/26). Persistent flow acceleration within the interior of the Greenland ice sheet. *Geophysical Research Letters*, *41*(3), 899–905. doi: 10.1002/2013GL058933
Enderlin, E. M., Howat, I. M., & Vieli, A. (2013). High sensitivity of tidewater outlet glacier dynamics to shape. *The Cryosphere*, *7*(3), 1007–1015. doi: 10.5194/tc-7-1007-2013
Enderlin, E. M., O'Neel, S., Bartholomaus, T. C., & Joughin, I. (2018). Evolving environmental and geometric controls on Columbia Glacier's continued retreat. *Journal of Geophysical Research: Earth Surface*, *123*, 1528 - 1545. doi: 10.1029/2017JF004541
ENVEO. (2017). *Greenland ice velocity map 2016/2017 from Sentinel-1 [version 1.0].* `http://products.esa-icesheets-cci.org/products/details/greenland_ice_velocity_map_winter_2016_2017_v1_0.zip/`.
Everett, A., Murray, T., Selmes, N., Holland, D., & Reeve, D. E. (2021). The impacts of a subglacial discharge plume on calving, submarine melting and mélange mass loss at Helheim Glacier, south east Greenland. *Journal of Geophysical Research: Earth Surface*, e2020JF005910. doi: 10.1029/2020JF005910
Felikson, D., A. Catania, G., Bartholomaus, T. C., Morlighem, M., & Noël,

B. P. Y. (2021). Steep glacier bed knickpoints mitigate inland thinning in Greenland. *Geophysical Research Letters*, *48*(2), e2020GL090112. doi: https://doi.org/10.1029/2020GL090112

Felikson, D., Bartholomaus, T. C., Catania, G. A., Korsgaard, N. J., Kjær, K. H., Morlighem, M., … Nash, J. D. (2017). Inland thinning on the Greenland ice sheet controlled by outlet glacier geometry. *Nature Geoscience*, *10*(5), 366–369. doi: 10.1038/ngeo2934

Fowler, A. C. (1982). Waves on glaciers. *Journal of Fluid Mechanics*, *120*, 283-321. doi: 10.1017/S0022112082002778

Fried, M. J., Catania, G. A., Stearns, L. A., Sutherland, D. A., Bartholomaus, T. C., Shroyer, E., & Nash, J. (2018). Reconciling drivers of seasonal terminus advance and retreat at 13 Central West Greenland tidewater glaciers. *Journal of Geophysical Research: Earth Surface*, *123*(7), 1590–1607. doi: 10.1029/2018JF004628

Howat, I. M., Ahn, Y., Joughin, I., van den Broeke, M. R., Lenaerts, J. T. M., & Smith, B. (2011). Mass balance of Greenland's three largest outlet glaciers, 2000–2010. *Geophysical Research Letters*, *38*(12), L12501. doi: 10.1029/2011GL047565

Howat, I. M., Joughin, I., & Scambos, T. A. (2007, 03). Rapid changes in ice discharge from Greenland outlet glaciers. *Science*, *315*(5818), 1559. doi: 10.1126/science.1138478

Howat, I. M., Joughin, I., Tulaczyk, S., & Gogineni, S. (2005). Rapid retreat and acceleration of Helheim Glacier, east Greenland. *Geophysical Research Letters*, *32*(22), L22502. doi: 10.1029/2005GL024737

Jenkins, A. (2011). Convection-driven melting near the grounding lines of ice shelves and tidewater glaciers. *Journal of Physical Oceanography*, *41*(12), 2279–2294. doi: 10.1175/JPO-D-11-03.1

Joughin, I., Das, S. B., King, M. A., Smith, B. E., Howat, I. M., & Moon, T. (2008). Seasonal speedup along the western flank of the Greenland Ice Sheet. *Science*, *320*(5877), 781–783. doi: 10.1126/science.1153288

Joughin, I., Howat, I. M., Smith, B., & Scambos, T. (2020). *MEaSUREs Greenland Ice Velocity: Selected Glacier Site Velocity Maps from InSAR, Version 3.* NASA National Snow and Ice Data Center Distributed Active Archive Center. Boulder, Colorado USA. doi: 10.5067/YXMJRME5OUNC

Joughin, I., Smith, B., Howat, I. M., Scambos, T., & Moon, T. (2010). Greenland flow variability from ice-sheet-wide velocity mapping. *Journal of Glaciology*, *56*(197), 415-430. doi: 10.3189/002214310792447734

Kamb, B., Engelhardt, H., Fahnestock, M. A., Humphrey, N., Meier, M., & Stone, D. (1994). Mechanical and hydrologic basis for the rapid motion of a large tidewater glacier: 2. Interpretation. *Journal of Geophysical Research: Solid Earth*, *99*(B8), 15231–15244. doi: 10.1029/94JB00467

Kehrl, L. M., Joughin, I., Shean, D. E., Floricioiu, D., & Krieger, L. (2017). Seasonal and interannual variabilities in terminus position, glacier velocity, and surface elevation at Helheim and Kangerlussuaq Glaciers from 2008 to 2016. *Journal of Geophysical Research: Earth Surface*, *122*(9), 1635–1652. doi: 10.1002/2016JF004133

Khan, S. A., Kjeldsen, K. K., Kjær, K. H., Bevan, S., Luckman, A., Aschwanden, A., … Fitzner, A. (2014). Glacier dynamics at Helheim and Kangerdlugssuaq glaciers, southeast Greenland, since the Little Ice Age. *The Cryosphere*, *8*(4), 1497–1507. doi: 10.5194/tc-8-1497-2014

King, M. D., Howat, I. M., Candela, S. G., Noh, M. J., Jeong, S., Noël, B. P. Y., … Negrete, A. (2020). Dynamic ice loss from the Greenland Ice Sheet driven by sustained glacier retreat. *Communications Earth & Environment*, *1*(1), 1. doi: 10.1038/s43247-020-0001-2

Krabill, W., Frederick, E., Manizade, S., Martin, C., Sonntag, J., Swift, R., … Yungel, J. (1999, 03). Rapid thinning of parts of the southern Greenland Ice Sheet. *Science*, *283*(5407), 1522. doi: 10.1126/science.283.5407.1522

Luckman, A., Benn, D. I., Cottier, F., Bevan, S., Nilsen, F., & Inall, M. (2015). Calving rates at tidewater glaciers vary strongly with ocean temperature. *Nature Communications*, *6*(1), 8566. doi: 10.1038/ncomms9566

Ma, Y., & Bassis, J. N. (2019). The effect of submarine melting on calving from marine terminating glaciers. *Journal of Geophysical Research: Earth Surface*, *124*(2), 334–346. doi: 10.1029/2018JF004820

Mankoff, K. D., Colgan, W., Solgaard, A., Karlsson, N. B., Ahlstrøm, A. P., van As, D., … Fausto, R. S. (2019). Greenland Ice Sheet solid ice discharge from 1986 through 2017. *Earth System Science Data*, *11*(2), 769–786. doi: 10.5194/essd-11-769-2019

Mankoff, K. D., Noël, B., Fettweis, X., Ahlstrøm, A. P., Colgan, W., Kondo, K., … Fausto, R. S. (2020). Greenland liquid water discharge from 1958 through 2019. *Earth System Science Data*, *12*(4), 2811–2841. doi: 10.5194/essd-12-2811-2020

Meier, M. F., Lundstrom, S., Stone, D., Kamb, B., Engelhardt, H., Humphrey, N., … Walters, R. (1994). Mechanical and hydrologic basis for the rapid motion of a large tidewater glacier: 1. Observations. *Journal of Geophysical Research: Solid Earth*, *99*(B8), 15219–15229. doi: 10.1029/94JB00237

Meier, M. F., & Post, A. (1987). Fast tidewater glaciers. *Journal of Geophysical Research: Solid Earth*, *92*(B9), 9051–9058. doi: 10.1029/JB092iB09p09051

Miller, O., Solomon, D. K., Miège, C., Koenig, L., Forster, R., Schmerr, N., … McConnell, J. R. (2020). Hydrology of a perennial firn aquifer in Southeast Greenland: An overview driven by field data. *Water Resources Research*, *56*(8), e2019WR026348. doi: 10.1029/2019WR026348

Moon, T., Joughin, I., & Smith, B. (2015). Seasonal to multiyear variability of glacier surface velocity, terminus position, and sea ice/ice mélange in northwest Greenland. *Journal of Geophysical Research: Earth Surface*, *120*(5), 818–833. doi: 10.1002/2015JF003494

Moon, T., Joughin, I., Smith, B., van den Broeke, M. R., van de Berg, W. J., Noël, B., & Usher, M. (2014). Distinct patterns of seasonal Greenland glacier velocity. *Geophysical Research Letters*, *41*(20), 7209–7216. doi: 10.1002/2014GL061836

Morlighem, M., Williams, C. N., Rignot, E., An, L., Arndt, J. E., Bamber, J. L., … Zinglersen, K. B. (2017). BedMachine v3: Complete bed topography and ocean bathymetry mapping of Greenland from multibeam echo sounding combined with mass conservation. *Geophysical Research Letters*, *44*(21), 11,051-11,061. doi: 10.1002/2017GL074954

Morlighem, M., Wood, M., Seroussi, H., Choi, Y., & Rignot, E. (2019). Modeling the response of northwest Greenland to enhanced ocean thermal forcing and subglacial discharge. *The Cryosphere*, *13*(2), 723–734. doi: 10.5194/tc-13-723-2019

Motyka, R. J., Hunter, L., Echelmeyer, K. A., & Connor, C. (2003). Submarine melting at the terminus of a temperate tidewater glacier, LeConte Glacier, Alaska, U.S.A. *Annals of Glaciology*, *36*, 57-65. doi: 10.3189/172756403781816374

Murray, T., Nettles, M., Selmes, N., Cathles, L. M., Burton, J. C., James, T. D., … Baugé, T. (2015, 07). Reverse glacier motion during iceberg calving and the cause of glacial earthquakes. *Science*, *349*(6245), 305. doi: 10.1126/science.aab0460

Murray, T., Scharrer, K., James, T. D., Dye, S. R., Hanna, E., Booth, A. D., … Huybrechts, P. (2010). Ocean regulation hypothesis for glacier dynamics in southeast Greenland and implications for ice sheet mass changes. *Journal of Geophysical Research: Earth Surface*, *115*(F3), F03026. doi:

10.1029/2009JF001522
Nettles, M., Larsen, T. B., Elósegui, P., Hamilton, G. S., Stearns, L. A., Ahlstrøm, A. P., ... Forsberg, R. (2008). Step-wise changes in glacier flow speed coincide with calving and glacial earthquakes at Helheim Glacier, Greenland. *Geophysical Research Letters*, *35*(24). doi: 10.1029/2008GL036127
Nick, F. M., Vieli, A., Howat, I. M., & Joughin, I. (2009). Large-scale changes in Greenland outlet glacier dynamics triggered at the terminus. *Nature Geoscience*, *2*(2), 110–114. doi: 10.1038/ngeo394
Nienow, P. W., Sole, A. J., Slater, D. A., & Cowton, T. R. (2017). Recent advances in our understanding of the role of meltwater in the Greenland Ice Sheet system. *Current Climate Change Reports*, *3*(4), 330–344. doi: 10.1007/s40641-017-0083-9
Noël, B., van de Berg, W. J., van Wessem, J. M., van Meijgaard, E., van As, D., Lenaerts, J. T. M., ... van den Broeke, M. R. (2018). Modelling the climate and surface mass balance of polar ice sheets using RACMO2 – Part 1: Greenland (1958–2016). *The Cryosphere*, *12*(3), 811–831. doi: 10.5194/tc-12-811-2018
Nowicki, S., Goelzer, H., Seroussi, H., Payne, A. J., Lipscomb, W. H., Abe-Ouchi, A., ... van de Wal, R. (2020). Experimental protocol for sea level projections from ISMIP6 stand-alone ice sheet models. *The Cryosphere*, *14*(7), 2331–2368. doi: 10.5194/tc-14-2331-2020
Nye, J. F. (1960). The response of glaciers and ice-sheets to seasonal and climatic changes. *Proceedings of the Royal Society of London A: Mathematical, Physical and Engineering Sciences*, *256*(1287), 559-584.
O'Leary, M., & Christoffersen, P. (2013). Calving on tidewater glaciers amplified by submarine frontal melting. *The Cryosphere*, *7*(1), 119–128. doi: 10.5194/tc-7-119-2013
O'Neel, S., Pfeffer, W. T., Krimmel, R., & Meier, M. (2005). Evolving force balance at Columbia Glacier, Alaska, during its rapid retreat. *Journal of Geophysical Research: Earth Surface*, *110*(F3), F03012. doi: 10.1029/2005JF000292
Parizek, B. R., & Alley, R. B. (2004). Implications of increased Greenland surface melt under global-warming scenarios: ice-sheet simulations. *Quaternary Science Reviews*, *23*(9), 1013–1027. doi: 10.1016/j.quascirev.2003.12.024
Phillips, T., Rajaram, H., & Steffen, K. (2010). Cryo-hydrologic warming: A potential mechanism for rapid thermal response of ice sheets. *Geophysical Research Letters*, *37*(20). doi: 10.1029/2010GL044397
Pimentel, S., & Flowers, G. E. (2011). A numerical study of hydrologically driven glacier dynamics and subglacial flooding. *Proceedings of the Royal Society A: Mathematical, Physical and Engineering Sciences*, *467*(2126), 537–558. doi: 10.1098/rspa.2010.0211
Podrasky, D., Truffer, M., Fahnestock, M., Amundson, J. M., Cassotto, R., & Joughin, I. (2012). Outlet glacier response to forcing over hourly to interannual timescales, Jakobshavn Isbræ, Greenland. *Journal of Glaciology*, *58*(212), 1212-1226. doi: 10.3189/2012JoG12J065
Poinar, K., Joughin, I., Lilien, D., Brucker, L., Kehrl, L., & Nowicki, S. (2017). Drainage of Southeast Greenland firn aquifer water through crevasses to the bed. *Frontiers in Earth Science*, *5*, 5. doi: 10.3389/feart.2017.00005
Reeh, N., & Olesen, O. B. (1986). Velocity measurements on Daugaard-Jensen Gletscher, Scoresby Sund, East Greenland. *Annals of Glaciology*, *8*, 146-150. doi: 10.3189/S0260305500001336
Riel, B., Minchew, B., & Joughin, I. (2021). Observing traveling waves in glaciers with remote sensing: new flexible time series methods and application to Sermeq Kujalleq (Jakobshavn Isbræ), Greenland. *The Cryosphere*, *15*(1), 407–429. doi: 10.5194/tc-15-407-2021
Rignot, E., Braaten, D., Gogineni, S. P., Krabill, W. B., & McConnell, J. R. (2004).

Rapid ice discharge from southeast Greenland glaciers. *Geophysical Research Letters*, *31*(10). doi: 10.1029/2004GL019474

Rignot, E., Fenty, I., Menemenlis, D., & Xu, Y. (2012). Spreading of warm ocean waters around Greenland as a possible cause for glacier acceleration. *Annals of Glaciology*, *53*(60), 257-266. doi: 10.3189/2012AoG60A136

Rignot, E., & Kanagaratnam, P. (2006). Changes in the velocity structure of the Greenland Ice Sheet. *Science*, *311*(5763), 986-990. doi: 10.1126/science.1121381

Rignot, E., Velicogna, I., van den Broeke, M. R., Monaghan, A., & Lenaerts, J. T. M. (2011). Acceleration of the contribution of the Greenland and Antarctic ice sheets to sea level rise. *Geophysical Research Letters*, *38*(5), L05503. doi: 10.1029/2011GL046583

Seabold, S., & Perktold, J. (2010). statsmodels: Econometric and statistical modeling with python. In *9th python in science conference.* doi: 10.25080/Majora-92bf1922-011

Shepherd, A., Hubbard, A., Nienow, P., King, M., McMillan, M., & Joughin, I. (2009). Greenland ice sheet motion coupled with daily melting in late summer. *Geophysical Research Letters*, *36*(1). doi: 10.1029/2008GL035758

Shumway, R. H., & Stoffer, D. S. (2017). *Time series analysis and its applications* (Fourth ed.). Cham, Switzerland: Springer.

Slater, D. A., Nienow, P. W., Cowton, T. R., Goldberg, D. N., & Sole, A. J. (2015). Effect of near-terminus subglacial hydrology on tidewater glacier submarine melt rates. *Geophysical Research Letters*, *42*(8), 2861–2868. doi: 10.1002/2014GL062494

Sole, A. J., Mair, D. W. F., Nienow, P. W., Bartholomew, I. D., King, M. A., Burke, M. J., & Joughin, I. (2011). Seasonal speedup of a Greenland marine-terminating outlet glacier forced by surface melt–induced changes in subglacial hydrology. *Journal of Geophysical Research: Earth Surface*, *116*(F3). doi: 10.1029/2010JF001948

Stearns, L. A., & Hamilton, G. S. (2007). Rapid volume loss from two East Greenland outlet glaciers quantified using repeat stereo satellite imagery. *Geophysical Research Letters*, *34*(5), L05503. doi: 10.1029/2006GL028982

Stevens, L. A., Behn, M. D., Das, S. B., Joughin, I., Noël, B. P. Y., van den Broeke, M. R., & Herring, T. (2016). Greenland Ice Sheet flow response to runoff variability. *Geophysical Research Letters*, *43*(21), 11,295–11,303. doi: 10.1002/2016GL070414

Todd, J., Christoffersen, P., Zwinger, T., Råback, P., Chauché, N., Benn, D., … Hubbard, A. (2018). A full-Stokes 3-D calving model applied to a large Greenlandic glacier. *Journal of Geophysical Research: Earth Surface*, *123*(3), 410–432. doi: 10.1002/2017JF004349

van der Veen, C. J. (2001). Greenland ice sheet response to external forcing. *Journal of Geophysical Research: Atmospheres*, *106*(D24), 34047–34058. doi: 10.1029/2001JD900032

van Dongen, E. C. H., Åström, J. A., Jouvet, G., Todd, J., Benn, D. I., & Funk, M. (2020). Numerical modeling shows increased fracturing due to melt-undercutting prior to major calving at Bowdoin Glacier. *Frontiers in Earth Science*, *8*, 253. doi: 10.3389/feart.2020.00253

Van Meijgaard, E., Van Ulft, L., Van de Berg, W., Bosveld, F., Van den Hurk, B., Lenderink, G., & Siebesma, A. (2008). *The KNMI regional atmospheric climate model RACMO version 2.1.* Koninklijk Nederlands Meteorologisch Instituut.

Vijay, S., Khan, S. A., Kusk, A., Solgaard, A. M., Moon, T., & Bjørk, A. A. (2019). Resolving seasonal ice velocity of 45 Greenlandic glaciers with very high temporal details. *Geophysical Research Letters*, *46*(3), 1485–1495. doi: 10.1029/2018GL081503

Virtanen, P., Gommers, R., Oliphant, T. E., Haberland, M., Reddy, T., Cournapeau, D., … SciPy 1.0 Contributors (2020). SciPy 1.0: Fundamental Algorithms for Scientific Computing in Python. *Nature Methods*, *17*, 261–272. doi: 10.1038/s41592-019-0686-2

Voytenko, D., Stern, A., Holland, D. M., Dixon, T. H., Christianson, K., & Walker, R. T. (2015). Tidally driven ice speed variation at Helheim Glacier, Greenland, observed with terrestrial radar interferometry. *Journal of Glaciology*, *61*(226), 301-308. doi: 10.3189/2015JoG14J173

Weertman, J. (1958). Traveling waves on glaciers. *IASH*, *47*, 162–168.

Weertman, J., & Birchfield, G. E. (1983). Basal water film, basal water pressure, and velocity of traveling waves on glaciers. *Journal of Glaciology*, *29*(101), 20–27.

Werder, M. A., Hewitt, I. J., Schoof, C. G., & Flowers, G. E. (2013). Modeling channelized and distributed subglacial drainage in two dimensions. *Journal of Geophysical Research: Earth Surface*, *118*(4), 2140–2158. doi: 10.1002/jgrf.20146

Supporting Information for "Statistical inference shows Helheim Glacier velocity response to runoff, terminus position, and topography"

Lizz Ultee[1,2], Denis Felikson[3], Brent Minchew[1], Leigh A. Stearns[4], Bryan Riel[1]

[1]Dept. of Earth, Atmospheric, and Planetary Sciences, Massachusetts Institute of Technology, Cambridge, MA, USA

[2]School of Earth & Atmospheric Sciences, Georgia Institute of Technology, Atlanta, GA, USA

[3]NASA Goddard Space Flight Center, Greenbelt, MD, USA

[4]Department of Geology, University of Kansas, Lawrence, KS, USA

Contents of this file

1. Figure S1

Additional Supporting Information (Files uploaded separately)

1. Caption for Dataset S1

Data Set S1. Terminus position of Helheim Glacier (2002-2019) in terms of a width-averaged distance from an upstream flux gate, identified from satellite imagery. We primarily use Moderate Imaging Spectroradiometer (MODIS) imagery, but incorporate Landsat and Sentinel-2 imagery when available. Terminus positions are derived manually until 2010 (Schild & Hamilton, 2013) and using an semi-automated technique thereafter (e.g. Foga et al., 2014).

References

Foga, S., Stearns, L. A., & van der Veen, C. (2014). Application of satellite remote sensing techniques to quantify terminus and ice mélange behavior at Helheim Glacier, East Greenland. *Marine Technology Society Journal*, *48*(5), 81–91. doi: 10.4031/MTSJ.48.5.3

Schild, K. M., & Hamilton, G. S. (2013). *Terminus position time series: Helheim and Kangerslugssuaq glaciers, Greenland.* National Science Foundation Arctic Data Center. Retrieved from https://arcticdata.io/catalog/view/doi%3A10.18739%2FA2W93G doi: 10.18739/A2W93G

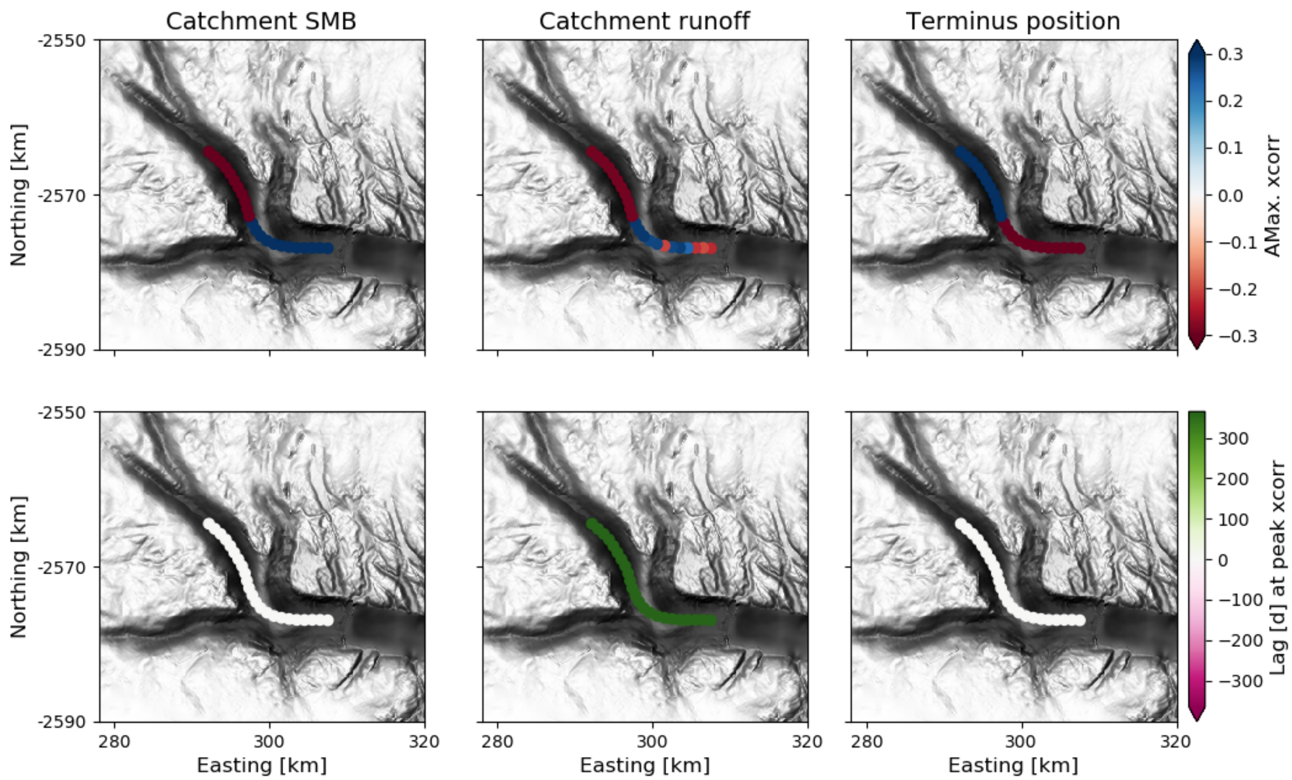

Figure S1. Cross-correlation of largest absolute value (top row) and corresponding lag (bottom row) between the long-term varying components of ice surface speed and each variable (columns). Colorbars for cross-correlation and lag used here are consistent with main text Figure 3 to allow intercomparison; however, the range of values represented here exceeds those shown on that figure.